From co-crystal to salt: The creation of four ternary co-crystals between benzoic acids and bipyridine through the combination of charge-transfer interactions and hydrogen bonding is reported (see figure). The altered crystal environment due to structural changes adjusts the level of proton transfer between the components. Thus, variation of a component can be used to convert a given pair from a co-crystal to a salt.

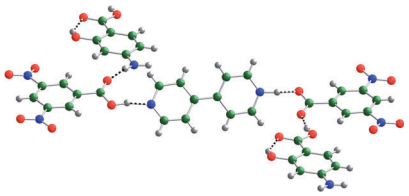

Crystal Engineering

C. C. Seaton, N. Blagden, T. Munshi, I. J. Scowen* ..... ▮▮▮▮–▮▮▮▮

Creation of Ternary Multicomponent Crystals by Exploitation of Charge-Transfer Interactions

CHEMISTRY
A EUROPEAN JOURNAL

ChemPubSoc
Europe

DOI: 10.1002/chem.201203578

Creation of Ternary Multicomponent Crystals by Exploitation of Charge-Transfer Interactions

Colin C. Seaton,*[a] Nicholas Blagden,[b] Tasnim Munshi,[c] and Ian J. Scowen[c]

Abstract: Four new ternary crystalline molecular complexes have been synthesised from a common 3,5-dinitrobenzoic acid (3,5-dnda) and 4,4′-bipyridine (bipy) pairing with a series of amino-substituted aromatic compounds (4-aminobenzoic acid (4-aba), 4-(*N*,*N*-dimethylamino)benzoic acid (4-dmaba), 4-aminosalicylic acid (4-asa) and sulfanilamide (saa)). The ternary crystals were created through the application of complementary charge transfer and hydrogen-bonding interactions. For these systems a dimer was created through a charge-transfer interaction between two of the components, while hydrogen bonding between the third molecule and this dimer completed the construction of the ternary co-crystal. All resulting structures display the same acid···pyridine interaction between 3,5-dnba and bipy. However, changing the third component causes the proton of this bond to shift from neutral OH···N to a salt form, $O^{-}\cdots HN^{+}$, as the nature of the group hydrogen bonding to the carboxylic acid was changed. This highlights the role of the crystal environment on the level of proton transfer and the utility of ternary systems for the study of this process.

Keywords: charge transfer · crystal engineering · hydrogen bonds · multicomponent crystals · X-ray diffraction

Introduction

The creation of multicomponent crystalline materials has recently been reinvigorated by the potential application of such materials as novel dosage forms for active pharmaceutical ingredients (APIs).[1] Although much activity has been undertaken on the creation of binary co-crystals, the creation of systems with three or more molecules (ternary or higher) is much less commonplace.[2] In the few examples available, ternary co-crystals have generally been created using a deliberate design strategy, but some have been formed serendipitously. For example, the complex between 2,4,6-trinitrobenzoic acid, 4-aminobenzoic acid and 1,3,5-trinitrobenzene[3] was isolated during the attempted co-crystallisation of 4-aminobenzoic acid and 2,4,6-trinitrobenzoic acid due to the decarboxylation of the trinitrobenzoic acid in water.

Strategies for the creation of ternary co-crystals include the partial replacement of one component in a known binary co-crystal by a similarly sized and shaped molecule[2k] or the introduction of a third component into voids within a binary co-crystal.[2i] The most commonly used strategy utilises a central linking molecule that can selectively hydrogen bond to the remaining components. This approach was pioneered by Aakeröy et al., initially with isonicotinamide and pairs of substituted benzoic acids.[2a–f] The ternary co-crystal is formed with the strongest acid (3,5-dinitrobenzoic acid (3,5-dnba)) selectively bonding to the best acceptor (pyridine nitrogen) and the weaker acid bonding to the weaker amide acceptor (Figure 1). Later work expanded on this through the development of novel linker molecules with differing N-heterocyclic groups. These were designed by consideration of the calculated molecular electrostatic potential, to selectively bind to different acid groups.[2h] Thus the selectivity of the interactions can be controlled by choosing functional groups to alter the strength of the hydrogen-bonding functionalities. However this requires a strong understand-

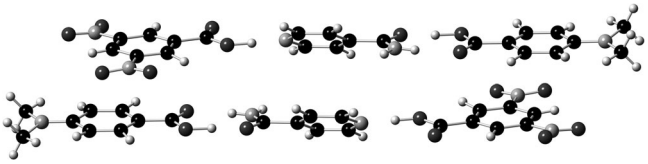

Figure 1. Bonding of components in the ternary complex between 3,5-dinitrobenzoic acid, 4-(dimethylamino)benzoic acid and isonicotinamide. Atom colouring: carbon, black; oxygen, dark grey; nitrogen, light grey; hydrogen, white.

[a] Dr. C. C. Seaton
Solid-State Pharmaceutical Cluster
Materials and Surface Science Institute
University of Limerick, Limerick (Ireland)
E-mail: colin.seaton@ul.ie

[b] Prof. N. Blagden
Lincoln School of Pharmacy
University of Lincoln, Brayford Pool
Lincoln, Lincolnshire, LN6 7TS (UK)

[c] Dr. T. Munshi, Prof. I. J. Scowen
Division of Chemical and Forensic Science
University of Bradford, Richmond Road
Bradford, BD7 1DP (UK)

Supporting information for this article is available on the WWW under http://dx.doi.org/10.1002/chem.201203578.

ing of the competition between potential hydrogen bonds. One way to expand this approach is to utilise complementary types of intermolecular interaction to bind the differing components together. Thus two components may be held together by hydrogen bonds and the third component can be bonded to this dimer by an alternative type such as a charge-transfer interaction. Charge-transfer interactions are commonly encountered as donor–acceptor interactions formed by the partial overlap of the HOMO and LUMO orbitals of the molecules. These orbitals must display similar energy and symmetry and are frequently exhibited between aromatic molecules with electron-donating groups (e.g., amine groups) and electron-withdrawing groups (e.g., nitro groups). The binary co-crystal formed between 3,5-dnba and 4-(*N*,*N*-dimethylamino)benzoic acid (4-dmaba) displays such a charge-transfer interaction (Figure 2a), which is retained

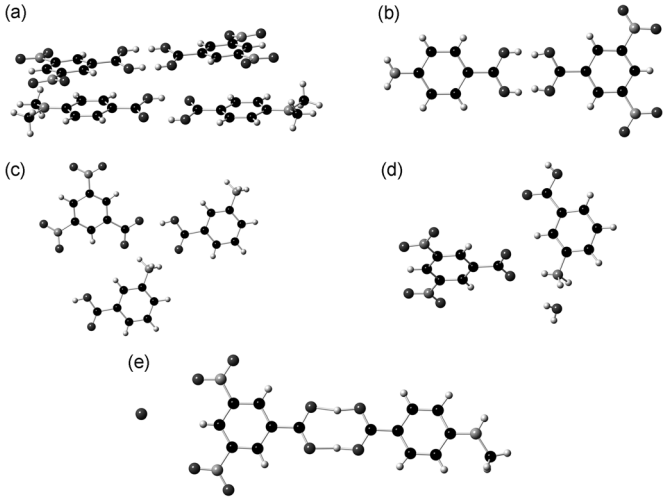

Figure 2. Hydrogen-bonding motifs in 3,5-dinitrobenzoic acid/aminobenzoic acid co-crystals: a) 4-(dimethylamino)benzoic acid, b) 4-aminobenzoic acid, c) 3-aminobenzoic acid, d) 3-aminobenzoic acid hydrate and e) 4-(methylamino)benzoic acid hydrate.

on creation of a ternary co-crystal with isonicotinamide (Figure 1) and salts of the co-crystal with lithium, sodium and ammonia,[4] thereby highlighting the robustness of this interaction. A number of binary co-crystals between 3,5-dnba and other aminobenzoic acids display such charge-transfer interactions (Figure 2)[5] and so these systems were chosen as two of the components of the systems studied to investigate the potential for ternary co-crystallisation through a combination of hydrogen bonding and charge-transfer interactions.

The carboxylic acid···pyridine hydrogen bond is a frequently utilised supramolecular synthon in crystal engineering[6] and offers a robust hydrogen bond to the benzoic acids selected previously. The symmetric 4,4′-bipyridine (bipy) molecule was selected as the final component of the systems studied, as this would offer two hydrogen-bond acceptors of equal strength and so differences in selectivity towards the acids would be driven by the differing strengths of two acid

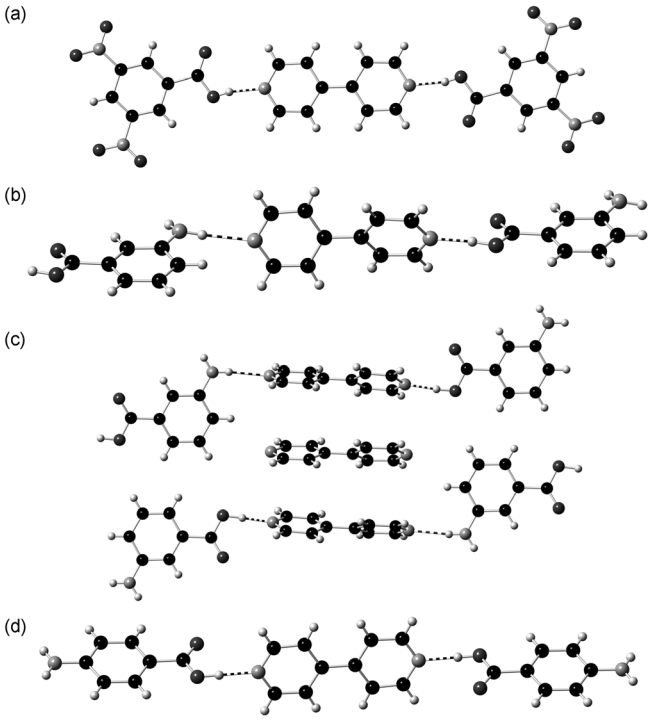

Figure 3. Hydrogen-bonding motifs between bipy and a) 3,5-dnba, b) 3-aba (1:1), c) 3-aba (3:2) and d) 4-aba.

groups. Binary co-crystals have been reported between bipy and 3,5-dnba (Figure 3a),[7] 3-aminobenzoic acid (3-aba, Figure 3b)[8] and 4-aminobenzoic acid (4-aba, Figure 3c),[8a,9] with the 3-aba system existing in both 1:1 and 3:2 compositions. As 3,5-dnba has the lowest pK_a of the benzoic acids considered, it would be expected to preferentially bind to the bipy. If a complex with an equimolar composition is formed, then the creation of a bilayered complex could be envisioned (Figure 4).

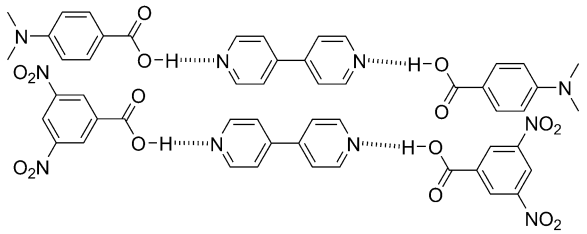

Figure 4. Proposed interaction between species within the ternary co-crystal shown for the 3,5-dnba/bipy/4-dmaba system.

The creation of ternary crystalline molecular complexes was initially undertaken between 3,5-dnba and bipy with 2-aminobenzoic acid (2-aba), 3-aba, 4-aba and 4-dmaba. To investigate the influence of the functional group on the observed interactions, 4-aminosalicylic acid (4-asa) and sulfanilamide (saa) were also tested. The ternary crystals were grown through solution crystallisation routes and the obtained materials were identified by single-crystal X-ray diffraction.

Results and Discussion

Complex 3,5-dnba/bipy/4-dmaba (I): The ternary complex **I** has a 2:1:2 (3,5-dnba/bipy/4-dmaba) composition despite being grown from a solution with an equimolar composition. The 3,5-dnba and bipy molecules are bound together by a $CO_2H\cdots N_{pyridine}$ hydrogen bond, while the charge-transfer interaction holds the 4-dmaba and 3,5-dnba molecules together (Figure 5). A second charge-transfer interaction occurs

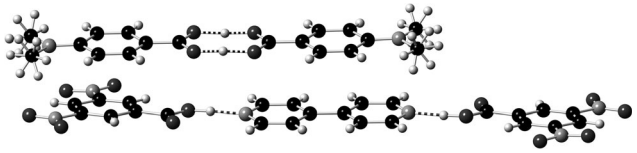

Figure 5. Packing of the three components in complex **I** (atom colouring as in Figure 1).

between the 4-dmaba and the bipy molecules between the amino N and the pyridine N. The expected addition of a second bipy molecule between the 4-dmaba dimers, however, does not occur. Instead the homo-molecular $R_2^2(8)$ hydrogen bond between the 4-dmaba molecules is maintained. The same interaction occurs in both the single-component phase and the binary complex with 3,5-dnba (Figure 1d). The level of proton disorder depends on the crystal state and has been investigated further by variable-temperature X-ray and neutron diffraction studies.[10] The creation of ternary co-crystals thus offers the possibility for future study into the role of the crystal structure upon proton disorder if the same hydrogen bond can be retained through a set of ternary co-crystals with variations in the third component. The three components form 2D sheets in the (203) plane through weak C–H···O=N interactions (Figure 6). The final crystal is formed from the stacking of these sheets along the *b* axis by the combination of charge-transfer and π···π interactions.

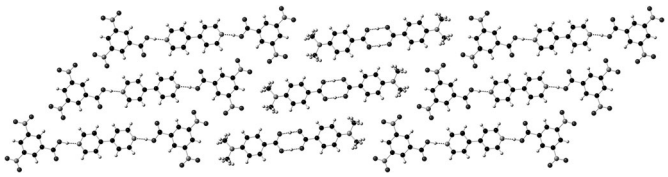

Figure 6. Formation of the 2D sheet structure in complex **I** through the combination of hydrogen-bonding interactions.

Complex 3,5-dbna/bipy/4-aba (II): Complex **II** has a 2:1:1 (3,5-dbna/bipy/4-aba) composition, again differing from the solution composition. The asymmetric unit cell of the structure contains two independent ternary fragments each with similar hydrogen bonding. The 3,5-dnba molecules again bind to the bipy molecules through $CO_2H \cdots N_{pyridine}$ hydrogen bonding. However, the two symmetry-independent pairs display differing levels of hydrogen disorder in these bonds. One appears to be a neutral pair with the hydrogen located close to the 3,5-dnba molecules on either side of the bipy. The other pair displays a more saltlike behaviour; the hydrogen is located either by the bipy nitrogen or located centrally in the bond (Figure 7). The oxygen to nitrogen distance for all four pairs is the same, whereas the carbon to oxygen bond lengths in the carbonyl fragments display the variation expected by the formation of neutral and salt structures (Table 1), however full confirmation would require neutron diffraction studies.

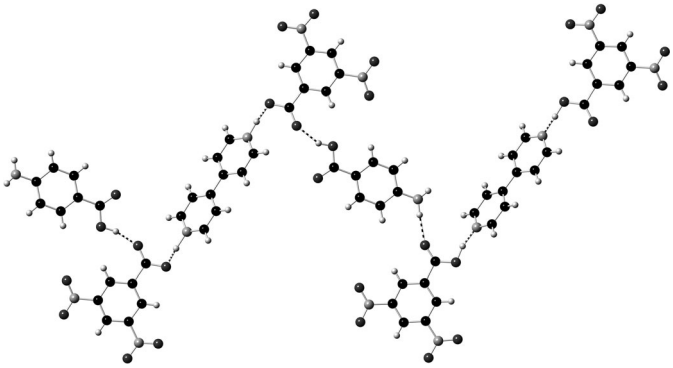

Figure 7. Asymmetric unit cell of complex **II** showing the differing hydrogen-bonding motifs of the 3,5-dnba molecules (atom colouring as in Figure 1).

Table 1. Bonds lengths for the carbonyl fragments in **II**.

Fragment	C=O [Å]	C–OH [Å]	O···N [Å]
$C_{7H}–O_{11H}O_{12H}$	1.207	1.288	2.548
$C_{7F}–O_{21F}O_{22F}$	1.218	1.285	2.544

The carbonyl oxygen of the neutral 3,5-dnba acts as a hydrogen-bond acceptor from the NH_2 group of 4-aba, while the carbonyl group of the deprotonated 3,5-dnba is an acceptor for the CO_2H group of 4-aba. This difference in interaction distinguishes the two 3,5-dnba/bipy dimers. The remaining hydrogen of the 4-aba functional group acts as a hydrogen-bond donor to the CO_2H group of a 4-aba molecule to form a C(8) motif along the *a* axis. The interactions between the 3,5-dnba/bipy dimers and this 4-aba chain form a ribbon structure. The final 3D structure is constructed through π···π and charge-transfer interactions between these ribbons.

Complex 3,5-dnba/bipy/saa (III): The ternary complex **III** has a 1:1:1 composition, in which 3,5-dnba binds to bipy through a discrete $CO_2H\cdots N_{pyridine}$ hydrogen bond and the sulfanilamide molecules form a homo-dimer by a $R_2^2(8)$ $NH_2\cdots O=S$ interaction. During the refinement of **III** a disordered proton site between the acid of the 3,5-dinitrobenzoic acid and the pyridine of bipy was indicated. The difference

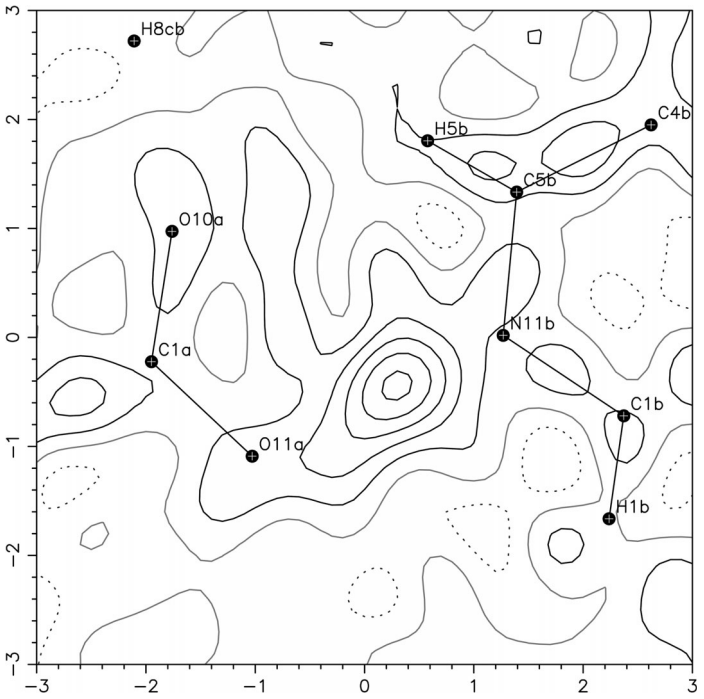

Figure 8. Fourier difference map for **III** showing the broad peak for the proton located between O3 and N1. A colour version of this graphic is available in the Supporting Information (Figure S1).

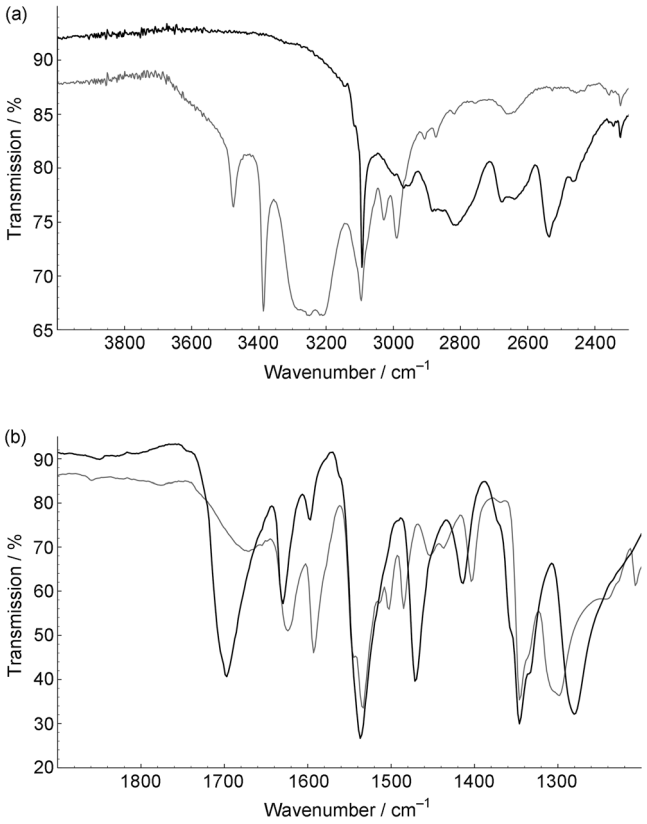

Figure 9. Infrared spectra for **III** (grey line) and 3,5-dnba (black line): a) N/O–H stretch and b) C=O stretch regions.

map between these sites was visualised in MapView within the program WinGX (Figure 8).[11] This indicated that the proton was bound to the nitrogen, although it is spread across a wide minimum. The infrared spectrum of this complex supports this interpretation, as it displays both a broad peak in the NH/OH stretch region (3300–3200 cm^{-1}, Figure 9a) and the shift in the C=O stretch to lower wavenumber compared to free 3,5-dnba (1698 to 1673 cm^{-1}, Figure 9b). These changes indicate the formation of a saltlike interaction between the carboxylic acid and the bipyridine. In this case the proton is transferred from the carboxylic acid to the bipyridine molecule to form a mixed co-crystal/salt. Once again the crystal-packing environment alters the level of proton disorder within the 3,5-dnba/bipy dimer.

Two 3,5-dnba/bipy dimers bind to the sulfanilamide dimer through a NH_2···O=C hydrogen bond forming a six-molecule cluster (Figure 10). These clusters form ribbon structures along the (110) axis through NH_2···O–N hydrogen bonds. These ribbons then form stacks along the *a* axis through NH_2···O–N hydrogen bonds. The final 3D structure is constructed by a stacking of the sheets along the *c* axis through weaker $C_{aromatic}$–H···$N_{pyridine}$, $C_{aromatic}$–H···O_{nitro} hydrogen bonds (Figure 11). Unlike the benzoic acid systems in which the amino and nitro groups lie parallel to each other, here the groups are perpendicular to each other (Figure 10), however the crystals do exhibit a yellow colouration suggesting some level of charge transfer.

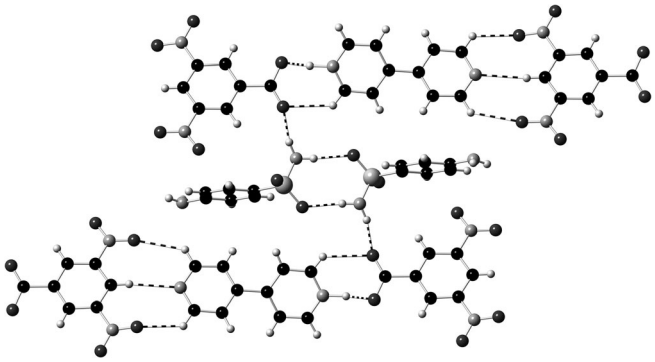

Figure 10. Packing of the three components in complex **III** (atom colouring as in Figure 1).

Complex 3,5-dnba/bipy/4-asa (IV): Ternary complex **IV** has a 2:1:1 composition with the two 3,5-dinitrobenzoic acid molecules bonding to both pyridine groups of the bipy molecule. However, the nature of the bond at either component differs. One end binds through a neutral O–H···N hydrogen bond, whereas at the other proton transfer has occurred resulting in an O^-···H–N^+ hydrogen bond. The difference in binding mode is reflected in the bond lengths of the carboxylic group (Table 2), while the secondary bonding environment of these groups is different as in **II**. Visualisation of the difference map at the protonated pyridine confirms the localisation of the proton on the nitrogen (Figure 12).

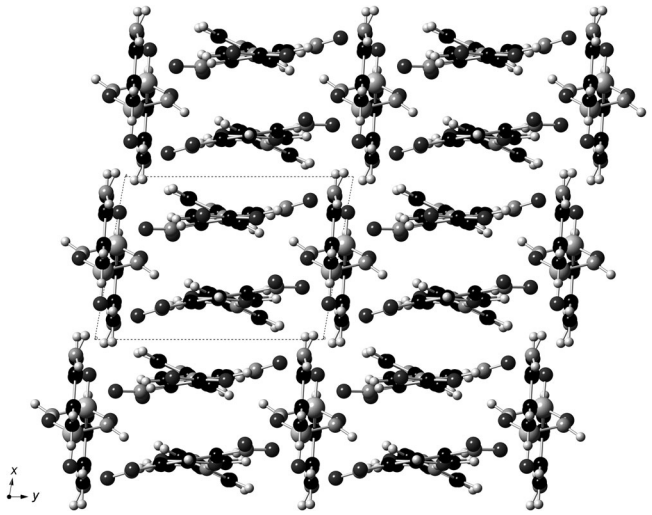

Figure 11. View along the *c* axis showing the formation of the 3D structure of complex **III**.

Table 2. Bonds lengths for the 3,5-dinitrobenzoic acid carbonyl fragments in **IV**.

Fragment	C=O [Å]	C–OH [Å]
C_{1A}–$O_{10A}O_{11A}$	1.225	1.306
C_{1B}–$O_{10B}O_{11B}$	1.249	1.271

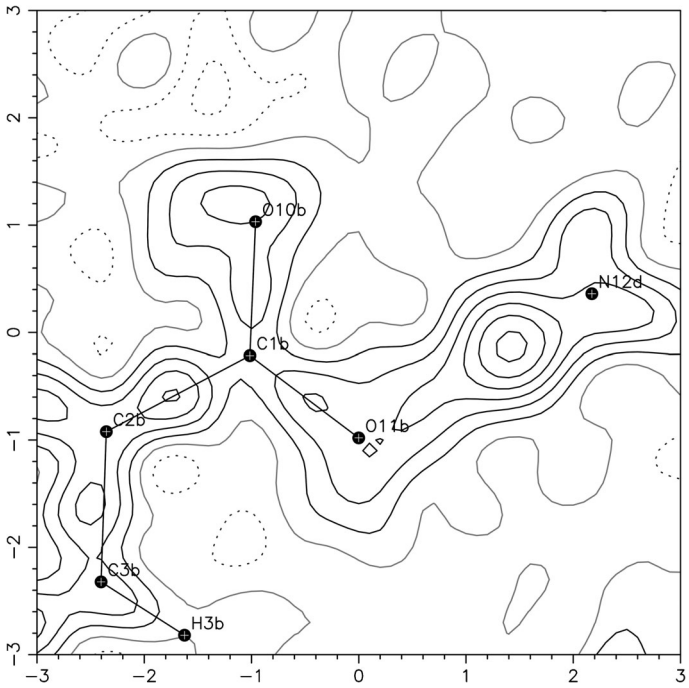

Figure 12. Fourier difference map of **IV** showing the greater localisation of the proton on the bipy nitrogen compared to the 3,5-dnba carboxylate oxygen ion. A colour version of this graphic is available in the Supporting Information (Figure S2).

Both carboxylic acid groups are involved in hydrogen bonds to 4-asa molecules: the neutral group forms a N–H···O hydrogen bond with one of the amino hydrogen atoms, while the deprotonated group forms an O–H···O hydrogen bond from the carboxylic acid group of 4-asa (Figure 13). These are the same interactions as in **II**, but in this case they occur on either side of the same bipy molecule, whereas in **II** they are bound to two different bipy molecules. The OH group on 4-asa forms an intramolecular hydrogen bond with the carboxylic acid group, while the remaining amine proton forms a N–H···O hydrogen bond with the carbonyl group of an 4-asa molecule resulting in a C(8) motif along the *c* axis, which then links the previously identified molecular clusters into the final 3D crystal structure.

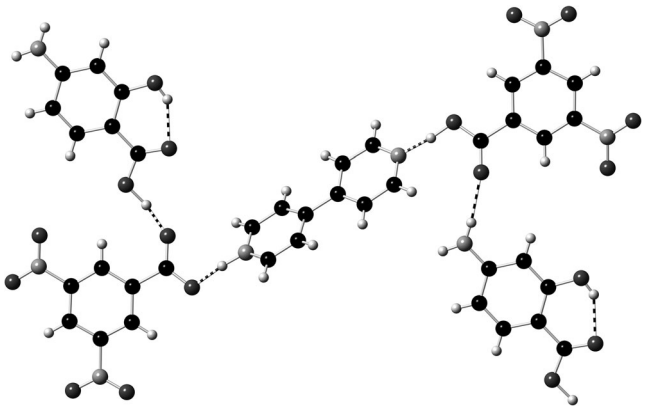

Figure 13. The hydrogen bonding between the molecular components in **IV** (atom colouring as in Figure 1).

Influence of growth conditions: The role of the growth conditions on the final crystal phase was investigated by undertaking a limited crystallisation screen by variation of the solvent (acetone, ethanol, nitromethane, acetonitrile) for systems **I** and **II**. The previously obtained ternary complex was obtained in most cases, either as the only product or a mixture with one of the binary complexes. The only exception was the 3,5-dnba/bipy/4-aba mixture from nitromethane that resulted in the binary 3,5-dnba/bipy co-crystal (Table 3).

Table 3. Results of the solvent screening.

System	Solvent	Product
3,5-dnba/bipy/4-dmaba	acetone	**I**
3,5-dnba/bipy/4-dmaba	ethanol	**I**
3,5-dnba/bipy/4-dmaba	nitromethane	3,5-dnba/bipy
3,5-dnba/bipy/4-dmaba	acetonitrile	**I**
3,5-dnba/bipy/4-aba	acetone	**II**
3,5-dnba/bipy/4-aba	ethanol	**II** + 3,5-dnba/bipy
3,5-dnba/bipy/4-aba	nitromethane	**II**
3,5-dnba/bipy/4-aba	acetonitrile	**II**

This indicates that the choice of solvent and changes in the solution speciation do not influence the level of proton transfer in the final crystal product. However, as with binary systems[12] the location of the region of thermodynamic stability of the multicomponent material varies with the solubility of the components.

Computational study: To support the experimental evidence for a charge-transfer interaction between the components and to identify whether the proton transfer observed within the system is due to the local chemical environment displayed within the crystal structure, a series of computational studies was carried out. The HOMO orbitals for 4-dmaba, 4-aba, saa and 4-asa and the LUMO orbitals for 3,5-dnba and 3,5-dnba/bipy dimer (with the hydrogen bonded to both oxygen and nitrogen) were calculated (Figure 14). Only the co-crystal form of the dimer displays a comparable symmetry and energy to the HOMO molecules and so charge-transfer interactions would only be expected in these cases. This is reflected in the crystal structures in which charge-transfer interactions are only observed in the co-crystal cases. The energetics of the observed interactions were investigated by DFT ab initio calculations. Optimisation of the charge-transfer acid pair confirms the stability of this interaction (Figure 15) and as expected this interaction is weaker than the hydrogen-bonding dimer (Table 4). For the 4-dmaba and 4-aba system trimer, formation strengthens both interactions, whereas for the 4-asa and saa systems this process weakens the bonds. This may be a reason why the stacked motif is not observed in the saa complex structure. However, the geometry obtained from the optimisation does display greater deviation from the experimental structure (Figure 16).

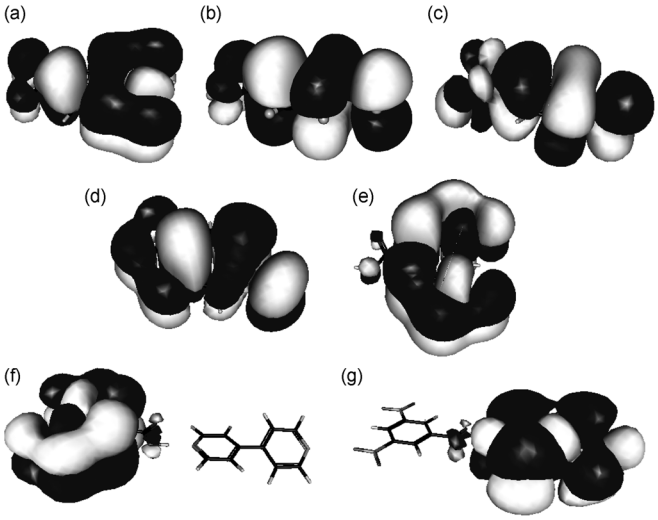

Figure 14. Calculated HOMO molecular orbitals for a) 4-dmaba, b) 4-aba, c) saa, d) 4-asa; and LUMO molecular orbitals for e) 3,5-dnba, f) 3,5-dnba/bipy co-crystal dimer and g) 3,5-dnba/bipy salt dimer. A colour version of this graphic is available in the Supporting Information (Figure S3).

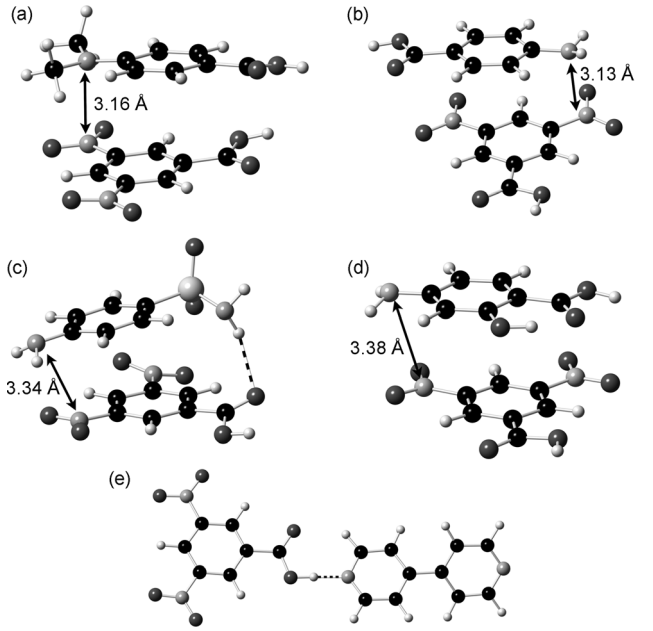

Figure 15. Optimised geometries of a) 4-dmaba/3,5-dnba, b) 4-aba/3,5-dnba, c) saa/3,5-dnba, d) 4-asa/3,5-dnba acid/acid CT dimers and e) the 3,5-dnba/bipy hydrogen-bond dimer. N-to-N distances are indicated for the acid/acid dimers.

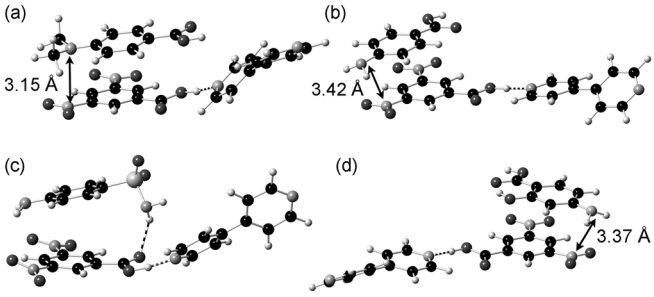

Figure 16. Optimised geometries for trimers between bipy and a) 4-dmaba/3,5-dnba, b) 4-aba/3,5-dnba, c) saa/3,5-dnba and d) 4-asa/35dnba. N-to-N distances are indicated for the benzoic acid/acid dimers.

Table 4. Energetics of the dimer and trimer formation.[a]

System	ΔE_{CT} dimer [kJ mol^{-1}]	$\Delta E_{H\ bond}$ dimer [kJ mol^{-1}]	ΔE_{CT} trimer [kJ mol^{-1}]	$\Delta E_{H\ bond}$ trimer [kJ mol^{-1}]
3,5-dnba/bipy/4-dmaba	−28.92	−58.13	−29.26	−58.46
3,5-dnba/bipy/4-aba	−25.24	−58.13	−27.50	−60.39
3,5-dnba/bipy/4-asa	−29.65	−58.13	−26.72	−55.20
3,5-dnba/bipy/saa	−28.77	−58.13	−22.64	−52.00

[a] For dimer energies, $\Delta E_{CT} = E_{CT\ dimer} - (E_{acid1} + E_{acid2})$, $\Delta E_{H\ bond} = E_{H\text{-}bond\ dimer} - (E_{acid1} + E_{bipy})$, whereas for trimer energies, $\Delta E_{CT} = E_{trimer} - (E_{H\text{-}bond\ dimer} + E_{acid2})$, $\Delta E_{H\ bond} = E_{trimer} - (E_{CT\ dimer} + E_{bipy})$.

Modelling of the energy landscape for the proton transfer between the 3,5-dnba/bipy molecules indicates that the local chemical environment adjusts both the position and shape of the minima in this case (Figure 17). For the isolated

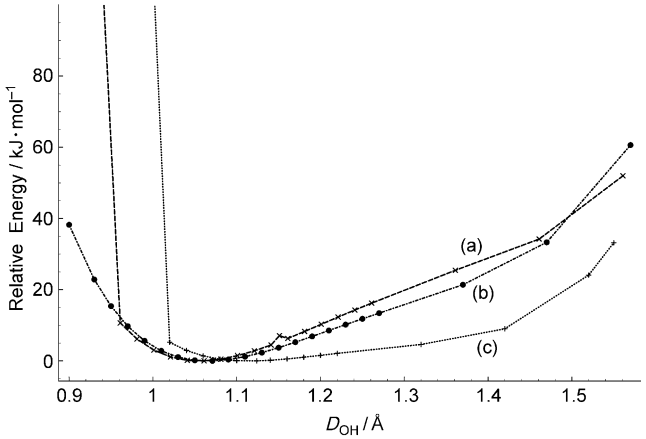

Figure 17. Calculated energy landscape for the gas-phase proton transfer between 3,5-dnba and bipy molecules: a) isolated dimer pair, b) trimer with 4-aba bonding through the NH_2 group and c) trimer with 4-aba bonding through the CO_2H group.

dimer, a minima with an O–H distance of 1.06 Å was located on a relatively narrow surface. The presence of a 4-aba molecule bonding through the carboxylic acid group shifts the minima to 1.12 Å and significantly broadens the minima out, which indicates a greater probability of proton movement. In contrast, the presence of 4-aba bonding through the amino hydrogen does not move the location of the hydrogen atom (1.07 Å) but again broadens the energy surface. Thus, even simple gas-phase calculations indicate that in these systems the presence of a strong acid functional group bonding onto the acid/pyridine dimer is enough to adjust the bonding preferences. Further study is required to see whether high-level solid-state calculations as applied to other systems support these conclusions.[13]

Conclusion

The successful creation and single-crystal structure determination of four ternary multicomponent crystals, which all utilise a combination of charge-transfer interactions and hydrogen bonding, has demonstrated a targeted route to new materials. Overall, the expected charge-transfer interactions were maintained, whereas the hydrogen bonding exhibited was complex dependent. In all of the co-crystals the strongest hydrogen-bond donor (3,5-dnba) binds to the strongest hydrogen-bond acceptor (bipy) as expected by Etter's rules. However, the nature of this hydrogen bond was found to vary depending on the third component. In cases in which the proton is located on the 3,5-dnba molecule, the third component either does not hydrogen bond to the carboxylic acid group of 3,5-dnba (4-dmaba) or donates a hydrogen from an amino group (4-asa, 4-aba). In contrast to when the proton is transferred to bipy, the third component has formed a hydrogen bond through donation of hydrogen from a carboxylic acid (4-aba, 4-asa) or sulfonamide group (saa). The change in interaction strength alters the donating ability of the 3,5-dnba group. Computational studies confirm the strength of both the charge-transfer and hydrogen-bonding interactions in these cases for both the dimer and trimer formation. Thus, the creation of such ternary co-crystals offers a route to investigate proton transfer within a selected hydrogen bond since it may be possible to construct the same hydrogen-bond interaction (same chemical environment) in different crystal structures. However, given the current inability to predict whether two molecules would successfully form a binary co-crystal, the designed creation of ternary co-crystals appears to still remain a significant challenge.

Experimental Section

Preparation of single crystals

Complex I: 3,5-Dinitrobenzoic acid (0.206 g, 1.0 mmol), 4-(dimethylamino)benzoic acid (0.157 g, 1 mmol) and 4,4′-bipyridine (0.183 g, 1.1 mmol) were dissolved in methanol (30 mL) with sufficient heating to ensure complete dissolution. The resulting yellow solution was left to cool to room temperature and red crystals of the complex were obtained.

Complex II: 3,5-Dinitrobenzoic acid (0.207 g, 1.0 mmol), 4-aminobenzoic acid (0.158 g, 1.0 mmol) and 4,4′-bipyridine (0.138 g, 1.0 mmol) were dissolved in methanol (30 mL) with heating. Upon cooling of the yellow solution to room temperature, orange crystals of the complex were produced.

Complex III: 3,5-Dinitrobenzoic acid (0.594 g, 2.8 mmol), sulfanilamide (0.426 g, 2.7 mmol) and 4,4′-bipyridine (0.510 g, 3 mmol) were dissolved individually in methanol (3×10 mL). The methanolic solutions were then mixed. Upon standing, a clear powder initially precipitated followed by the formation of yellow block crystals of the ternary complex.

Complex IV: 3,5-Dinitrobenzoic acid (0.169 g, 0.8 mmol), 4-aminosalicylic acid (0.234 g, 1.0 mmol) and 4,4′-bipyridine (0.147 g, 1 mmol) were dissolved together in methanol (30 mL) with gentle heating. Upon cooling to room temperature yellow crystals of the ternary complex were obtained.

Complex V: 3,5-Dinitrobenzoic acid (0.239 g, 1.1 mmol), 2-aminobenzoic acid (0.200 g, 1.2 mmol) and 4,4′-bipyridine (0.150 g, 1.1 mmol) were dissolved individually in methanol (3×10 mL). The methanolic solutions were mixed and upon standing colourless block crystals were obtained.

Complex VI: 3,5-Dinitrobenzoic acid (0.168 g, 0.08 mmol), 3-aminobenzoic acid (0.278 g, 2 mmol) and 4,4′-bipyridine (0.232 g, 1 mmol) were dissolved individually in methanol (3×10 mL). The methanolic solutions were mixed and upon standing colourless block crystals were obtained.

Characterisation: For both systems **V** and **VI**, initially colourless crystals were formed and were identified as the 3,5-dinitrobenzoic acid/4,4′-bipyridine binary complex by powder X-ray diffraction (PXRD). Upon standing, orange-yellow crystals were produced during which time the crystals of the binary complex dissolved. Crystal structure analysis indicated that the crystal features a channel structure built from the 3,5-dinitrobenzoic acid/4,4-bipyridine complex with a disordered species within the channel. Further study is currently underway to fully identify this material. Differential scanning calorimetry (DSC) and thermogravimetric analysis (TGA) on all the samples indicated that they decomposed before melting.

Infrared spectra were collected on a ThermoNicolet Avatar 360 ESP FTIR with Golden Gate ATR attachment using the Omnic software for

Table 5. Crystallographic details for single-crystal structure determinations.[18]

	I	II	III	IV
formula	$C_{10}H_{10}N_2{\cdot}2(C_7H_4N_2O_6){\cdot}2(C_9H_{10}NO_2)$	$C_{10}H_{10}N_2{\cdot}C_{10}H_8N_2{\cdot}2(C_7H_4N_2O_6){\cdot}2(C_7H_3N_2O_6){\cdot}2(C_7H_7NO_2)$	$C_7H_3N_2O_6{\cdot}C_{10}H_9N_2{\cdot}C_6H_8N_2O_2S$	$C_7H_4N_2O_6{\cdot}C_7H_3N_2O_6{\cdot}C_{10}H_9N_2{\cdot}C_7H_6NO_3$
M_r	910.80	1435.13	540.52	733.56
crystal system	triclinic	monoclinic	triclinic	monoclinic
space group	$P\bar{1}$	$P2_1/n$	$P\bar{1}$	$P2_1/c$
T [K]	296	296	100	296
a [Å]	7.8741(2)	13.9354(3)	6.9161(3)	19.0085(9)
b [Å]	8.6773(3)	24.3274(6)	9.7440(4)	12.0413(7)
c [Å]	15.6094(5)	18.7646(5)	17.9311(6)	13.7850(7)
α [°]	80.213(2)	90	78.098(3)	90
β [°]	81.932(2)	92.218(1)	87.768(3)	90.755(2)
γ [°]	88.145(2)	90	79.210(4)	90
V [Å^3]	1040.56(6)	6356.7(3)	1161.50(8)	3154.9 (3)
Z	1	4	2	4
μ [mm^{-1}]	0.114	0.121	0.204	0.13
crystal size [mm]	$0.25\times0.18\times0.14$	$0.62\times0.20\times0.15$	$0.45\times0.35\times0.30$	$0.34\times0.31\times0.24$
reflns measured	44095	189236	7922	88362
independent reflns	4766	9834	4098	7516
reflns obsd ($I>2\sigma(I)$)	2503	6697	3285	6140
R_{int}	0.0460	0.044	0.026	0.030
$R(F^2>2\sigma(F^2))$	0.0465	0.045	0.0376	0.047
$wR(F^2)$	0.1136	0.167	0.1040	0.152
S	0.967	1.03	1.04	1.01
no. reflns	4766	9834	4098	7516
no. params	306	977	423	494
no. restraints	0	0	0	4
largest diff. peak, hole [e Å^{-3}]	0.155, −0.171	0.25, −0.18	0.50, −0.51	0.52, −0.24

collection and processing. DSC and TGA data were collect using TA instruments Q2000 and Q5000, respectively.

Single-crystal structure determination: The crystallographic details for all co-crystals are given in Table 5. The data for **I**, **II** and **IV** was collected on a Bruker X8 Apex II diffractometer using graphite monochromated $Mo_{K\alpha}$ radiation at 296 K. The data was collected and reduced using Bruker SMART software.[14] The structures of **I** and **II** were solved and refined using ShelxTL, whereas the structure of **IV** was solved and refined in Olex2[15] using ShelxS 97 and ShelxL 97.[16] The data for **III** was collected on an Oxford Diffraction Xcalibur using graphite monochromated $Mo_{K\alpha}$ radiation at 100 K. The data was collected and reduced using CrysAlisPro; the structures were solved using ShelxS 97 and refined in Crystals.[17]

Crystal growth conditions screening of I and II: 3,5-dnba (0.212 g, 1.0 mmol), bipy (0.156 g, 1.0 mmol) and the relevant aminobenzoic acid (4-dmaba (0.165 g, 1.0 mmol) or 4-aba (0.165 g, 0.7 mmol)) were dissolved with heating in the selected solvent (30 mL; acetone, ethanol, nitromethane or acetonitrile). The solutions were left to slowly cool and the final crystalline product was collected and identified through PXRD.

Computational methodology: The molecular structures of 3,5-dnba, 4-aba, 4-asa and saa were initially optimised at the DFT level of theory with a dispersion correction term (PBE-D3) in the ab initio program orca[19] using the AccOpt option (PBE-D3/TZVPP).[20] The orbitals of the HOMO and LUMO of each system were then calculated at the RI-B2PLYP/def2-QZVPP(-g,-f) level using the RI approximation.[20] Dimers of 3,5-dnba/bipy were constructed from the crystal structure in both the salt and co-crystal conformation; optimisation of all hydrogen atoms except that involved in the acid···pyridine interaction was carried out with a DFT calculation (PBE-D3/TZVP) and the orbitals were subsequently determined at the RI-B2PLYP/def2-QZVPP(-g,-f) level. Calculations of the acid/acid dimers and trimers were performed on clusters extracted from the crystal structures. The clusters were initially optimised using a DFT calculation (PBE-D3/TZVP) followed by single-point energy calculations at the RI-B2PLYP/def2-QZVPP(-g,-f) level. The 3,5-dnba/bipy dimer and two 3,5-dnba/bipy/4-aba trimers were extracted from the crystal structure and all the hydrogen atoms were optimised in a DFT calculation at the PBE-D3/TZVP level. The energy surface for the proton transfer from 3,5-dnba to bipy was then constructed by calculation of the energy of various structures as the proton was moved between the molecules. The energy calculations were carried out at the PBE-D3/TZVPP level.[20]

Acknowledgements

Dr. Chris Muryn (University of Manchester) is thanked for his help with the collection of the data for sample **III**. Computational portions of this work were undertaken as part of the Solid State Pharmaceutical Cluster supported by the Science Foundation Ireland (grant: 07/SRC/B1158).

[1] a) S. L. Morissette, O. Almarsson, M. L. Peterson, J. F. Remenar, M. J. Read, A. V. Lemmo, S. Ellis, M. J. Cima, C. R. Gardner, *Adv. Drug Delivery Rev.* **2004**, *56*, 275; b) O. Almarsson, M. J. Zaworotko, *Chem. Commun.* **2004**, 1889–1896; c) A. V. Trask, W. D. S. Motherwell, W. Jones, *Chem. Commun.* **2004**, 890; d) P. Vishweshwar, J. A. McMahon, M. L. Peterson, M. B. Hickey, T. R. Shattock, M. J. Zaworotko, *Chem. Commun.* **2005**, 4601–4603; e) P. Vishweshwar, J. A. McMahon, J. A. Bis, M. J. Zaworotko, *J. Pharm. Sci.* **2006**, *95*, 499; f) S. L. Childs, G. P. Stahly, A. Park, *Mol. Pharm.* **2007**, *4*, 323–338; g) N. Blagden, M. de Matas, P. T. Gavan, P. York, *Adv. Drug Delivery Rev.* **2007**, *59*, 617–630; h) C. B. Aakeröy, M. E. Fasulo, J. Desper, *Mol. Pharm.* **2007**, *4*, 317–322; i) W. W. Porter III, S. C. Elie, A. J. Matzger, *Cryst. Growth Des.* **2008**, *8*, 14; j) N. Shan, M. J. Zaworotko, *Drug Discovery Today* **2008**, *13*, 440–446; k) D. J. Berry, C. C. Seaton, W. Clegg, R. W. Harrington, S. J. Coles, P. N. Horton, M. B. Hursthouse, R. Storey, W. Jones, T. Friscic, N. Blagden, *Cryst. Growth Des.* **2008**, *8*, 1697–1712; l) S. L. Childs, N. Ro-

drigeuz-Horendo, L. S. Reddy, A. Jayasankar, C. Maheshwari, L. McCausland, R. Shipplett, B. C. Stahly, *CrystEngComm* **2008**, *10*, 856–864.

[2] a) C. B. Aakeröy, A. M. Beatty, B. A. Helfrich, *Angew. Chem.* **2001**, *113*, 3340–3342; *Angew. Chem. Int. Ed.* **2001**, *40*, 3240–3242; b) C. B. Aakeröy, J. Desper, J. F. Urbina, *Chem. Commun.* **2005**, 2820–2822; c) C. B. Aakeröy, J. Desper, J. F. Urbina, *Cryst. Growth Des.* **2005**, *5*, 1283; d) C. B. Aakeröy, D. J. Salmon, *CrystEngComm* **2005**, *7*, 439–448; e) C. B. Aakeröy, A. M. Beatty, K. Lorimer, *Mol. Cryst. Liq. Cryst.* **2006**, *456*, 163–174; f) C. B. Aakeröy, J. Desper, M. M. Smith, *Chem. Commun.* **2007**, 3936–3938; g) B. R. Bhogala, S. Basavoju, A. Nangia, *CrystEngComm* **2005**, *7*, 551–562; h) B. R. Bhogala, S. Basavoju, A. Nangia, *Cryst. Growth Des.* **2005**, *5*, 1683; i) T. Friscic, A. V. Trask, W. Jones, W. D. S. Motherwell, *Angew. Chem.* **2006**, *118*, 7708–7712; *Angew. Chem. Int. Ed.* **2006**, *45*, 7546–7550; j) B. R. Bhogala, A. Nangia, *New J. Chem.* **2008**, *32*, 800–807; k) S. Tothadi, A. Mukherjee, G. R. Desiraju, *Chem. Commun.* **2011**, *47*, 12080.

[3] D. E. Lynch, G. Smith, K. A. Byriel, C. H. L. Kennard, *Chem. Commun.* **1992**, 300–301.

[4] a) C. C. Seaton, I. J. Scowen, N. Blagden, *CrystEngComm* **2009**, *11*, 1793–1795; b) S. Bukenya, T. Munshi, I. J. Scowen, R. Skyner, D. A. Whitaker, C. C. Seaton, *CrystEngComm* **2013**, *15*, 2241–2250.

[5] a) A. M. Hindawey, A. M. G. Nassar, R. M. Issa, *Acta Chim. Acad. Sci. Hung.* **1977**, *92*, 263; b) A. M. Hindawey, A. M. G. Nassar, R. M. Issa, *Indian J. Chem. Sect. A: Inorg. Bio-inorg. Phys. Theor.* **1980**, *19A*, 615; c) M. C. Etter, G. M. Frankenbach, *Chem. Mater.* **1989**, *1*, 10–12; d) C. V. K. Sharma, K. Panneerselvam, T. Pilati, G. R. Desiraju, *J. Chem. Soc. Perkin Trans. 2* **1993**, 2209–2216; e) D. E. Lynch, G. Smith, K. A. Byriel, C. H. L. Kennard, *Aust. J. Chem.* **1994**, *47*, 1789–1798; f) V. R. Pedireddi, J. PrakashaReddy, *Tetrahedron Lett.* **2002**, *43*, 4927–4930; g) A. Parkin, C. C. Seaton, N. Blagden, C. C. Wilson, *Cryst. Growth Des.* **2007**, *7*, 531–534; h) K. Chadwick, G. Sadiq, R. J. Davey, C. C. Seaton, R. G. Pritchard, A. Parkin, *Cryst. Growth Des.* **2009**, *9*, 1278–1279.

[6] a) J. A. Bis, P. Vishweshwar, D. Weyna, M. J. Zaworotko, *Mol. Pharm.* **2007**, *4*, 401–416; b) T. R. Shattock, K. K. Arora, P. Vishweshwar, M. J. Zaworotko, *Cryst. Growth Des.* **2008**, *8*, 4533–4545; c) A. Lemmerer, N. B. Báthori, S. A. Bourne, *Acta Cryst. B* **2008**, *64*, 780–790; d) C. C. Seaton, A. Parkin, C. C. Wilson, N. Blagden, *Cryst. Growth Des.* **2009**, *9*, 47–56; e) N. B. Báthori, A. Lemmerer, G. A. Venter, S. A. Bourne, M. R. Caira, *Cryst. Growth Des.* **2011**, *11*, 75–87.

[7] a) V. R. Pedireddi, A. Ranganathan, S. Chatterjee, *Tetrahedron Lett.* **1998**, *39*, 9831–9834; b) C. J. Burchell, C. Glidewell, A. J. Lough, G. Ferguson, *Acta Cryst. B* **2001**, *57*, 201–212; c) T.-F. Tan, J. Han, M-L. Pang, H-B. Song, Y-X. Ma, J-B. Meng, *Cryst. Growth Des.* **2006**, *6*, 1186–1193.

[8] a) D. E. Lynch, S. Chatwin, S. Parsons, *Cryst. Eng.* **1999**, *2*, 137–144; b) P. Lhengwan, S. Achiwawanich, T. Duangthongyou, *Acta Cryst. Sect. E: Struct. Rep. Online* **2012**, *68*, o2569.

[9] R. H. Wang, F. L. Jiang, Y. F. Zhou, L. Han, M. C. Hong, *Inorg. Chim. Acta* **2005**, *358*, 545–554.

[10] L. H. Thomas, N. Blagden, M. J. Gutmann, A. A. Kallay, A. Parkin, C. C. Seaton, C. C. Wilson, *Cryst. Growth Des.* **2010**, *10*, 2770–2774.

[11] L. J. Farrugia, *J. Appl. Cryst.* **1999**, *32*, 837.

[12] a) D. H. Leung, S. Lohani, R. G. Ball, N. Canfield, Y. Wang, T. Rhodes, A. Bak, *Cryst. Growth Des.* **2012**, *12*, 1254; b) A. Ainouz, J.-R. Authelin, P. Billot, H. Lieberman, *Int. J. Pharm.* **2009**, *374*, 82–89; c) R. A. Chiarella, R. J. Davey, M. L. Peterson, *Cryst. Growth Des.* **2007**, *7*, 1223–1226.

[13] a) D. M. S. Martins, D. S. Middlemiss, C. R. Pulham, C. C. Wilson, M. T. Weller, P. F. Henry, N. Shankland, K. Shankland, W. G. Marshall, R. M. Ibberson, *J. Am. Chem. Soc.* **2009**, *131*, 3884–3893; b) D. S. Middlemiss, M. Facchini, C. A. Morrison, C. C. Wilson, *CrystEngComm* **2007**, *9*, 777–785; c) S. Mohamed, D. A. Tocher, M. Vickers, P. G. Karamertzanis, S. L. Price, *Cryst. Growth Des.* **2009**, *9*, 2881–2889.

[14] APEX2, Bruker AXS Inc., Madison, WI, **2005**.

[15] O. V. Dolomanov, L. J. Bourhis, R. J. Gildea, J. A. K. Howard, H. Puschmann, *J. Appl. Cryst.* **2009**, *42*, 339–341.

[16] G. M. Sheldrick, *Acta Cryst. Sect. A* **2008**, *64*, 112.

[17] P. W. Betteridge, J. R. Carruthers, R. I. Cooper, K. Prout, D. J. Watkin, *J. Appl. Cryst.* **2003**, *36*, 1487.

[18] CCDC-848555 (Complex **I**), CCDC-848556 (Complex **II**), CCDC-848557 (Complex **III**) and CCDC-848558 (Complex **IV**) contain the supplementary crystallographic data for this paper. These data can be obtained free of charge from The Cambridge Crystallographic Data Centre via www.ccdc.cam.ac.uk/data_request/cif.

[19] F. Neese, *WIREs Comput Mol Sci* **2012**, *2*, 73–78.

[20] a) A. Schäfer, H. Horn, R. Ahlrichs, *J. Chem. Phys.* **1992**, *97*, 2571; b) F. Weigend, R. Ahlrichs, *Phys. Chem. Chem. Phys.* **2005**, *7*, 3297. The Ahlrichs (2d,2p) polarisation functions were obtained from the TurboMole basis set library under ftp.chemie.uni-karlsruhe.de/pub/basen; c) S. Grimme, J. Antony, S. Ehrlich, H. Krieg, *J. Chem. Phys.* **2010**, *132*, 154104; d) F. Weigend, F. Furche, R. Ahlrichs, *J. Chem. Phys.* **2003**, *119*, 12753.

Received: October 8, 2012
Revised: May 15, 2013
Published online: ■■ ■■, 0000

